Supporting Information for

Vertical Heterostructures of Layered Metal Chalcogenides by van der Waals Epitaxy

*Xingwang Zhang,[†,‡] Fei Meng,[†] Jeffrey R. Christianson,[†] Christian Arroyo-Torres,[†] Mark A. Lukowski,[†] Dong Liang,[†] J. R. Schmidt,[†] Song Jin[†]**

[†] Department of Chemistry, University of Wisconsin-Madison, 1101 University Avenue, Madison, Wisconsin 53706, United States

[‡] Key Laboratory of Biomass Chemical Engineering of Ministry of Education, Department of Chemical Engineering and Biological Engineering, Zhejiang University, Hangzhou 310027, China

* E-mail: jin@chem.wisc.edu

I. Experimental and Theoretical Calculation Details

1. Chemicals and Materials

Sulfur powder (99.5%), selenium powder (99.5%), $MoCl_5$ (95%), and WCl_6 (99.9%) were purchased from Sigma-Aldrich and used without further purification. Fluorine-doped tin oxide (FTO) coated glass substrates (TEC 15) were bought from Hartford Glass.

2. Synthesis of SnS_2 Microplates

SnS_2 microplates were synthesized by thermal sulfurization of FTO glass substrates in a quartz tube (1 inch I.D.), which was connected to an Argon gas inlet and a vacuum pump and placed in a tube furnace (Thermal Fisher, Linderberg Blue). In a typical synthesis, an alumina boat containing 1.0 g sulfur powder was placed near the entrance of the tube just outside the heating zone of the tube furnace. The FTO substrates were placed at the center of the furnace. The tube was first evacuated to a base pressure of 10 mTorr and flushed three times with Ar before heating up. When the temperature reached 525–575 ℃, the boat was moved into the

heating zone that was at a temperature of 200–250 ℃. The sulfur vapor was carried downstream by an Ar flow of 50 sccm to react with the FTO on glass for 10 min. The temperature was then brought down to 300 ℃ while the Ar flow was increased to 125 sccm to remove the residual sulfur on the substrates for another 10 min. Finally the tube was cooled naturally to room temperature.

3. Synthesis of MoS_2-SnS_2, WS_2-SnS_2, and WSe_2-SnS_2 Heterostructures

The MoS_2-SnS_2 heterostructures were synthesized using a chemical vapor deposition (CVD) method. In a typical synthesis, a quartz tube (1 inch I.D.) was first treated with a Zerostat gun for 2 min to remove the electrostatically absorbed water on the wall. It was then connected to Ar and H_2 gas inlets and a vacuum pump, and placed in a tube furnace (Thermal Fisher, Linderberg Blue). A piece of glass substrate covered with as-grown SnS_2 plates without any pre-treatments was placed parallel to the tube at the center of the furnace. Two alumina boats containing 10 mg $MoCl_5$ and 0.4 g sulfur powder, respectively, were placed side by side near the entrance of the tube with the boat of $MoCl_5$ sitting at more upstream position just outside the heating zone and the boat of sulfur sitting just inside the furnace about 250 ℃. This created a sulfur atmosphere in the tube before the CVD reaction started, preventing the direct reaction between $MoCl_5$ and SnS_2 before the reaction between $MoCl_5$ and sulfur. During the deposition process, the distances between $MoCl_5$/sulfur boats and the SnS_2 substrate at the center of the furnace were about 12 and 8 cm, respectively. Without the protection of excess sulfur vapor, the SnS_2 microplates were severely etched as shown in Figure S2. $MoCl_5$ must be weighed in a glove box and rapidly sealed into the tube reactor to avoid hydrolysis in the air. The tube was first evacuated to a base pressure of 10 mTorr and flushed three times with Ar. Then the reaction zone was heated to 420–470 ℃ under an Ar flow of 125 sccm at 780 Torr, before both boats were moved into the heating zone to initiate the reaction, where the boat of $MoCl_5$ was at about 150–200 ℃ and sulfur at about

350-400 ℃. After reaction for 2–6 minutes, the temperature was then brought down to 300 ℃ while maintaining the Ar flow at 125 sccm for another 10 min to remove the residual sulfur on the growth substrate. Finally the tube was cooled naturally to room temperature. A control sample of MoS_2 nanostructures on a silicon/SiO_2 substrate was also synthesized under the same conditions as above and the reaction time was 4 minutes.

The synthetic procedures for WS_2-SnS_2 and WSe_2-SnS_2 heterostructures are similar to those for MoS_2-SnS_2. For the WS_2-SnS_2 heterostructures, 10 mg WCl_6 and 0.4 g S were used, the deposition temperature was 420–490 ℃ and the reaction time was 180 s. For the WSe_2-SnS_2 heterostructures, 10 mg WCl_6 and 0.4 g Se were used with the Se boat at the center of the tube furnace. The deposition temperature was 450 ℃ and the reaction time was 180 s with an addition of 1.0 sccm H_2 flow. All reaction occurred under an Ar flow of 125 sccm at 780 Torr.

4. Structural Characterization

Scanning electron microscopy (SEM) was performed using a LEO SUPRA 55 VP field-emission scanning electron microscope operated at 1 kV. To prepare the specimen for transmission electron microscope (TEM) and STEM imaging, the as-grown substrates were immersed in 2 mL of ethanol and sonicated for 1 min. The resulting suspension was drop casted onto a piece of TEM grid (Ted Pella, lacey carbon type-A support film, 300-mesh, copper, #01890-F). The cross sectional TEM samples were prepared by microtomy, where the as-grown SnS_2-MoS_2 heterostructures were first embedded in a polymer resin and then cut into thin slices with a thickness of 80 to 100 nm and glued onto copper grids. TEM and STEM-EDS mapping were carried out on a FEI Titan scanning transmission electron microscope at an accelerating voltage of 200 kV. The Raman spectra and photoluminescence (PL) of the samples were collected with an Aramis Confocal Raman Microscope using a 532

nm laser source and CCD detector. The spatial resolution was about 1 μm. A 1800 l/mm grating and a 100 μm aperture were applied. For PL experiments, the as-grown microplates were transferred onto the surface of silicon substrates covered with SiO_2 (330nm) by a drop cast method similar to the TEM sample preparation. For the sharp peaks in the 540−562 nm region that originate from Raman resonances, the positions of these Raman peaks expressed in wavenumbers of the Raman shift can be calculated using the equation: $\Delta\,\omega(cm^{-1}) = (\frac{1}{\lambda_0(nm)} - \frac{1}{\lambda_1(nm)}) \times \frac{(10^7 nm)}{cm}$, where λ_0 is the excitation wavelength, and λ_1 is the Raman spectrum wavelength, and the Raman shifts are consistent with those of the reported values.

5. Computational Methods

Geometries were constructed within the Atomistic Simulation Environment (ASE).[S1] A bilayer heterostructure was constructed consisting of one layer that is a 6 × 6 supercell of SnS_2 and a second layer that is a 7 × 7 supercell of MoS_2. In order to accurately model the 2-dimensional character of the heterostructures, interactions with its periodic images in the third dimension were minimized by including a vacuum gap of 10 Å. VASP calculations with the PBE exchange-correlation potential were performed using projector augmented waves (PAW)[S2,3] to describe the interactions between core and valence electrons. Since they consist of supercells of each of the pure materials, the heterostructures have large unit cells (about 2.2 nm in the lateral dimension and at least 1.9 nm in the vertical direction); therefore, the Brillouin zone was sampled only at the gamma point. A dipole correction was applied in the z-direction. Geometry optimizations were performed using the conjugate-gradient method implemented in VASP and were considered converged when the absolute value of the maximum force was less than 0.01 eV/Å. The total system and projected DOS were all generated using VASP using the default radius for each atom type. Output files from the VASP projected DOS for 3-L and 5-L structures were parsed for visualization using an

in-house code that was implemented into ASE. Charge densities of particular bands were visualized by projection into a small atomic basis set, as has been described previously.[S4]

II. Other Typical SEM Image of SnS_2 Microplates

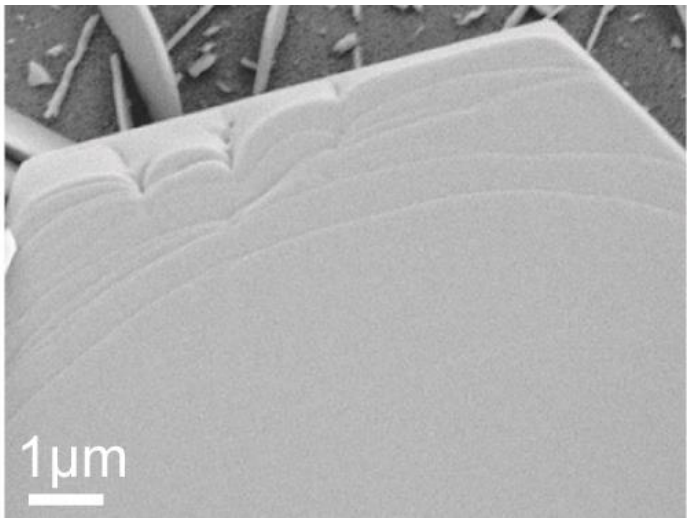

Figure S1. Other example SEM image of SnS_2 microplate. This image clearly shows the layered structure of a SnS_2 microplate.

III. The Etching Effect of $MoCl_5$ on SnS_2 Microplates

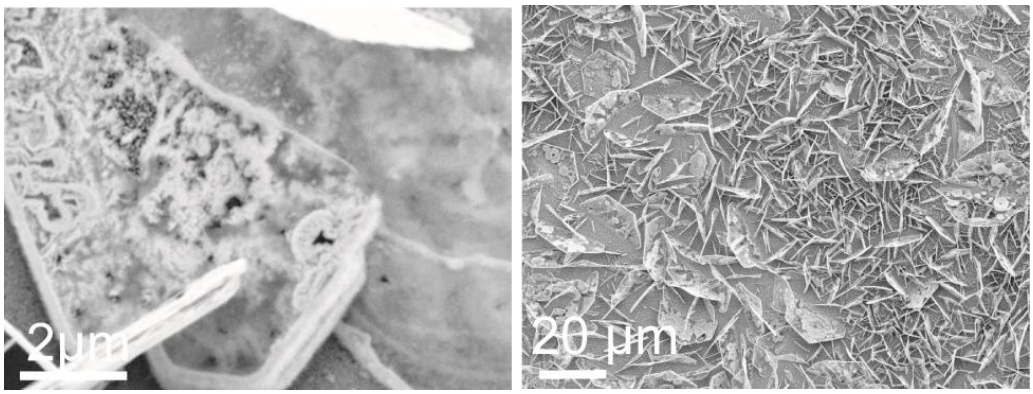

Figure S2. The SEM images showing severe etching of the SnS_2 microplates after CVD of MoS_2, if insufficient amount of sulfur precursor was used. Exact conditions: $MoCl_5$ (10 mg), sulfur powder (50 mg), Ar flow (125 sccm), temperature (450 ℃), reaction time (3 min).

IV. SEM Images and Raman Spectra of MoS_2-SnS_2 Heterostructures Prepared at 405 ℃ and 490 ℃

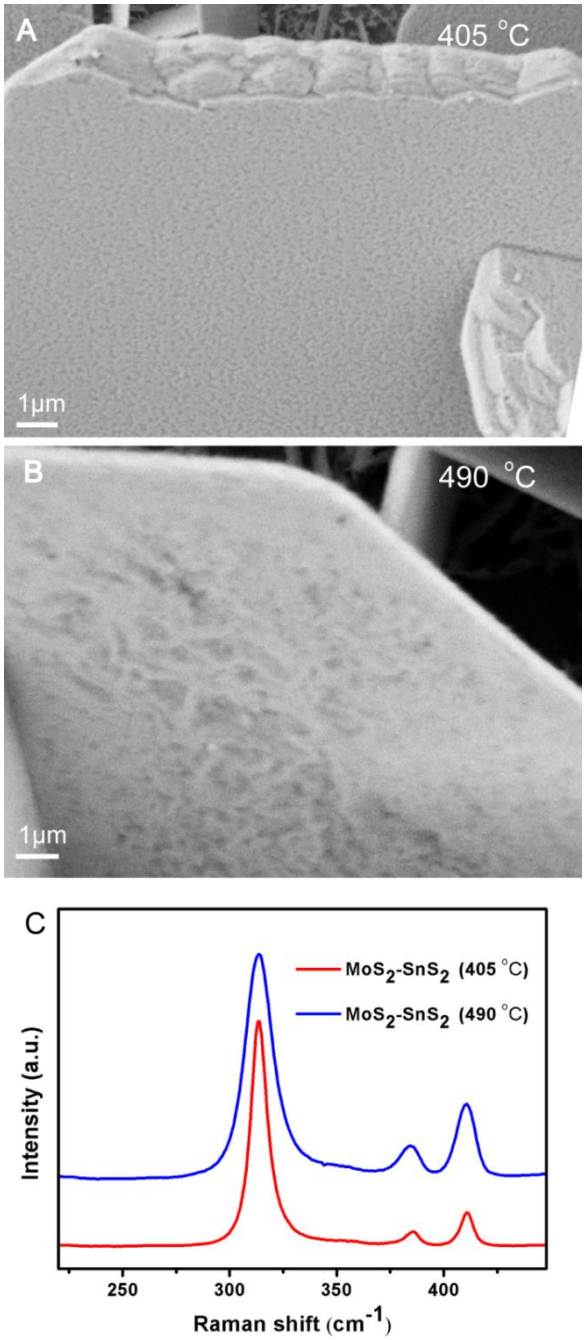

Figure S3. Representive SEM images of MoS_2-SnS_2 heterostructures grown at a deposition temperature of 405 ℃ (A) and 490 ℃ (B). (C) Raman spectra of these MoS_2-SnS_2 samples. Other conditions: $MoCl_5$ (10 mg), sulfur (0.4 g), Ar flow (125 sccm), reaction time (4 min).

V. SEM Images and Raman Spectra of WS_2-SnS_2 Heterostructures Prepared at 420 ℃ and 490 ℃

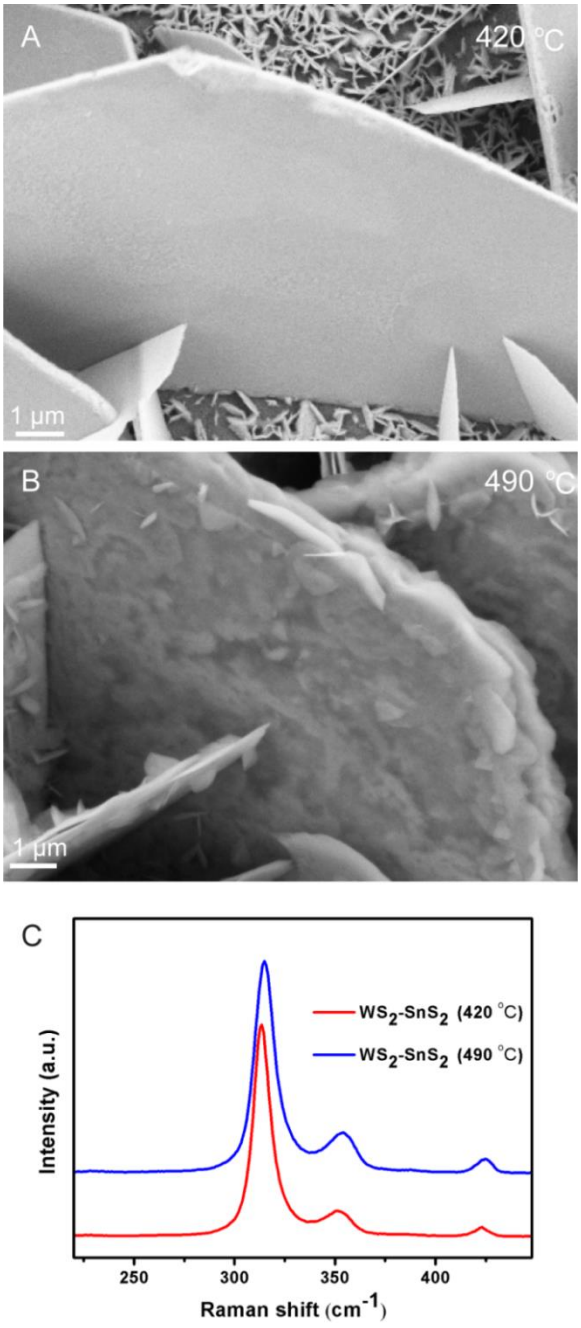

Figure S4. The SEM images of WS_2-SnS_2 heterostructures with a deposition temperature of 420 ℃ (A) and 490 ℃ (B). (C) Raman spectra of WS_2-SnS_2 samples. Other conditions: WCl_6 (10 mg), sulfur (0.4 g), Ar flow (125 sccm), reaction time (3 min).

VI. A Typical SEM Image of SnS_2 after a CVD Reaction at 650 ℃ Using MoO_3 as Precursor

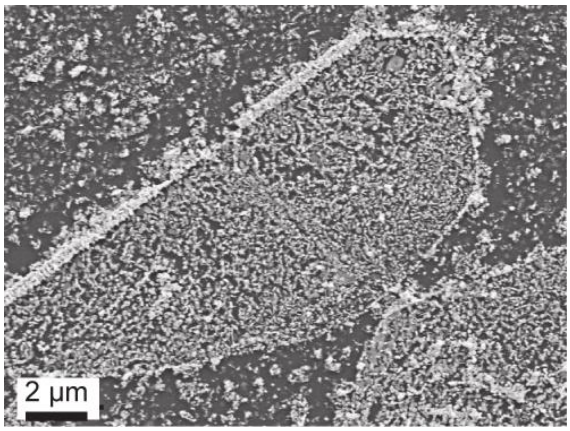

Figure S5. SEM image showing the decomposition of SnS_2 microplates after CVD of MoS_2 using MoO_3 as precursor at a high temperature 650 ℃. Conditions: MoO_3 (0.4 mg), sulfur powder (0.8 g), Ar flow (50 sccm), reaction time (3 min).

VII. Profiles of Lattice Fringes of MoS_2 Overgrowth Layer and Additional Cross Sectional TEM Image.

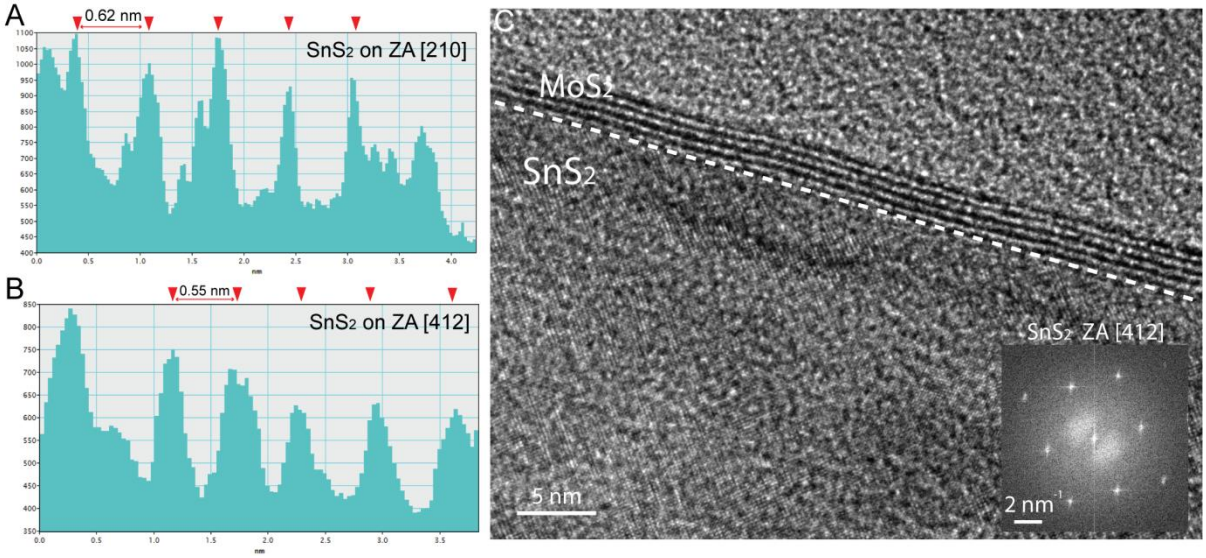

Figure S6. TEM profiles showing the MoS_2 layer spacing (A and B) and additional cross sectional TEM image (C) of MoS_2-SnS_2 heterostructures. (A) Lattice fringe profile of MoS_2

layers shown in Figure 3A in the main text, which matches well with the ideal (002) lattice spacing of MoS_2. (B) Lattice fringe profile of MoS_2 layers shown in panel C, which shows smaller apparent spacing due to a view angle not along the basal plane. (C) Cross sectional TEM image of another MoS_2-SnS_2 heterostructure observed along the [412] zone axis of SnS_2. The inset shows the FFT of the SnS_2 crystal that can be indexed to be along the [412] zone axis, which is not parallel to the basal plane of the hexagonal crystal structures for SnS_2 and MoS_2. Despite this, it still can be seen that five layers of MoS_2 are stacked on top of the SnS_2 crystals. However, the apparent spacings observed for the MoS_2 layers (0.55 nm by profile, Figure S6B) are smaller than the actual layer spacing of 0.615 nm, because the viewing angle is not directly end-on to the *c* planes and the projection of the atomic columns necessarily results in apparently smaller observed lattice spacing.

VIII. Confirmation of Single Crystalline MoS_2 Growth on SnS_2 Plates.

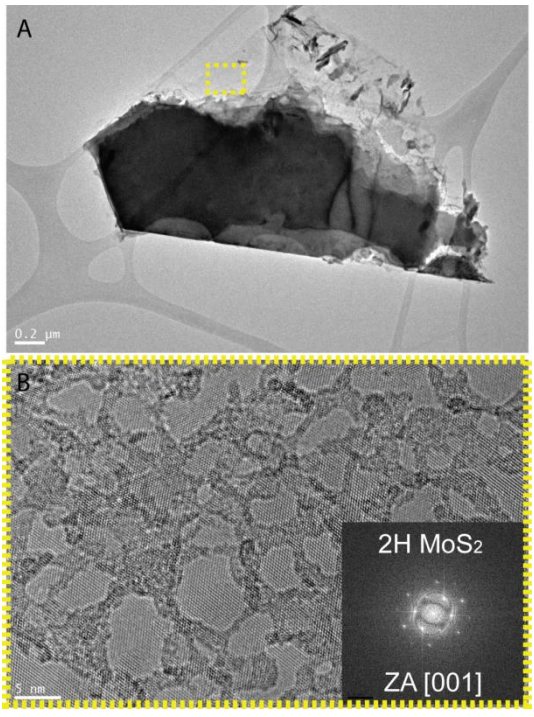

Figure S7. TEM and HRTEM confirming the single crystallinity of the MoS_2 layer in

MoS_2-SnS_2 heterostructures. (A) Low-resolution TEM of one heterostructure sample showing the extended growth of MoS_2 at the edge of the plate without the support of the SnS_2 plate. (B) The corresponding lattice-resolved HRTEM image for the yellow dashed box region in (A), where only few-layer MoS_2 is present. The corresponding FFT (inset) can be clearly indexed to 2H-MoS_2 with a zone axis of [001] perpendicular to the layer.

IX. Confirmation of Uniform and Complete Coverage of MoS_2 on SnS_2

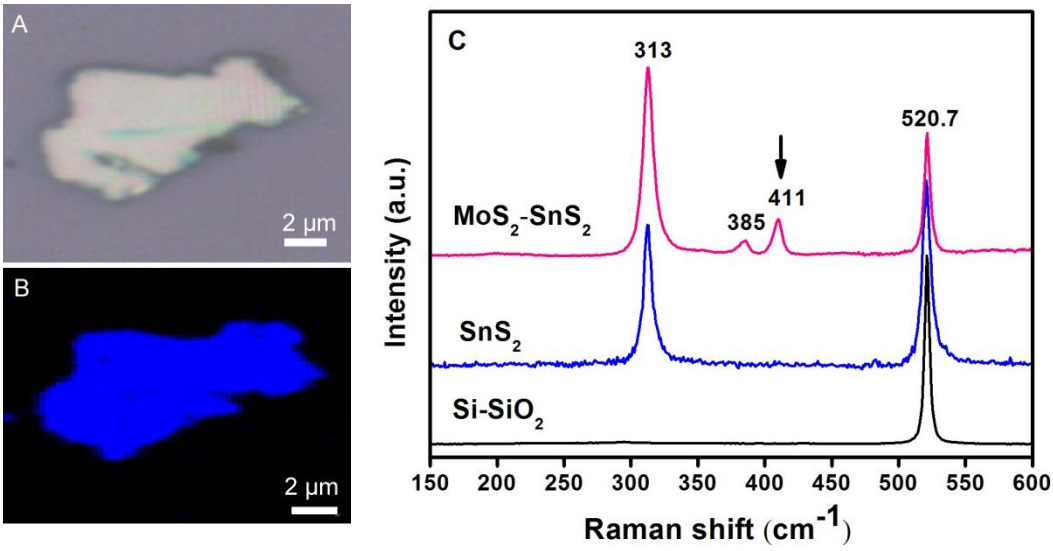

Figure S8. Confirmation of uniform and complete coverage of MoS_2 on SnS_2 surface by Raman mapping. (A) Optical micrograph of a single MoS_2-SnS_2 plate mechanically removed and deposited on a silicon/SiO_2 substrate; (B) the Raman mapping image of the same MoS_2-SnS_2 plate by using A_{1g} Raman peak of MoS_2 (411 cm^{-1}, marked with an arrow in C); (C) the red curve is a representative Raman spectrum of the same MoS_2-SnS_2 plate shown in A, the blue curve is a representative Raman spectrum of a single SnS_2 plate on silicon/SiO_2 substrate, the black curve is a representative Raman spectrum on the Si/SiO_2 substrate without MoS_2-SnS_2 plates. The peaks at 313 and 520.7 cm^{-1} are attributed to SnS_2 and Si,

respectively. The peaks at 385 and 411 cm^{-1} are the E^1_{2g}, A_{1g} peaks of MoS_2, respectively. The Raman spectra are consistent with what are shown in Figure 2E in the main text.

X. Photoluminescence Spectrum of MoS_2

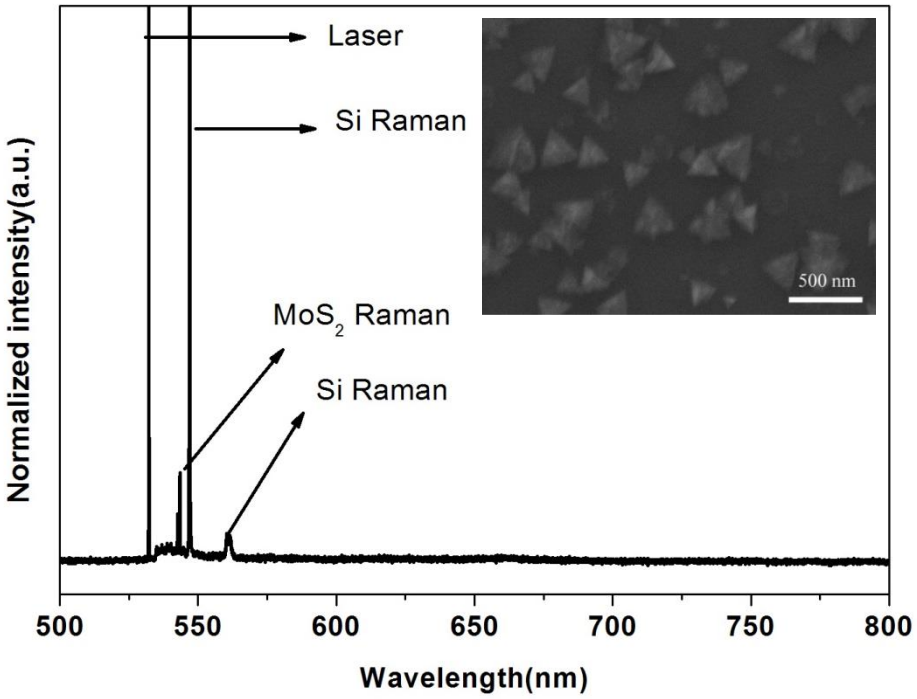

Figure S9. A representative PL spectrum of MoS_2 on a silicon/SiO_2 substrate made using identical reaction conditions as the MoS_2-SnS_2 heterostructure samples in Figure 3. No obvious features besides the MoS_2 and Si Raman peaks are observed. Inset shows a SEM image of the MoS_2 products.

XI. More Details on the Electronic Structure Calculations

Figure S10 demonstrates how the layering of the heterostructures influences the DOS. Comparing 1-L and 2-L structures where the nearest MoS_2-SnS_2 layer center to layer center distance is 12.5 Å (Figure S10a and S10b), the effect of homo-layer coupling is observed,

since the projected DOS is strictly a superposition of the DOS of each material. A broadening of the peaks is observed, but the peak positions do not change appreciably. On the other hand, comparing the DOS for the separated (Figure S10a) and interacting 1-L structures at the optimized distances of 6.2 Å (layer center to layer center) (Figure S10c) shows the effect of hetero-layer coupling. The total DOS for the interacting structure is largely the same as the DOS for the separated structure except in the regions where both SnS_2 and MoS_2 have DOS at similar energies and therefore couple, such as in the enlarged regions shown in Figure S10.

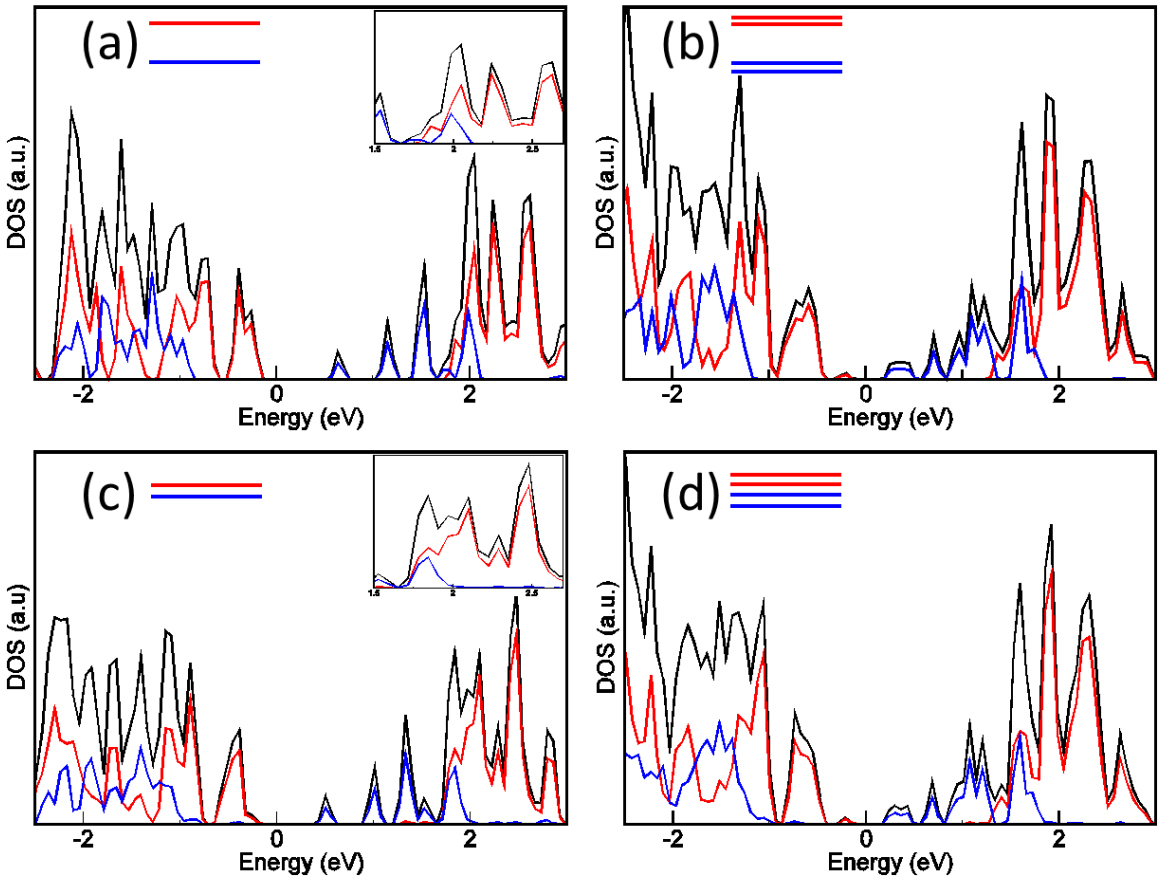

Figure S10. Total (black) and projected (MoS_2-red and SnS_2-blue) DOS for 1-L (a and c) and 2-L (b and d) structures where the layered materials are separated by a vacuum gap of 10 Å (a and b) and at their optimized distances of 6.2 Å (c and d) such that they are interacting.

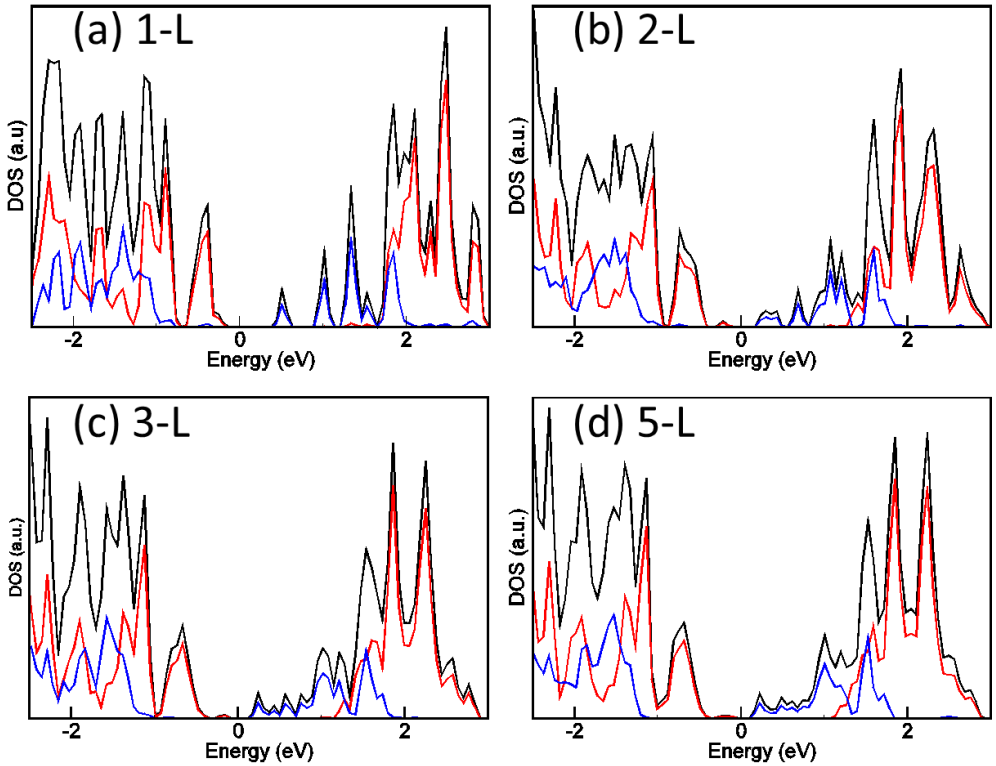

Figure S11. Total (black) and projected (MoS_2-red and SnS_2-blue) DOS for 1-L (a), 2-L (b), 3-L (c), and 5-L (d) structures showing the convergence of the DOS with respect to the number of layers. Panel (d) shows the same DOS highlighted in Figure 5B in the main text.

References:

(S1) Bahn, S. R.; Jacobsen, K. W. An Object-Oriented Scripting Interface to a Legacy Electronic Structure Code. *Computing in Science & Engineering* **2002**, *4*, 56-66.

(S2) Blöchl, P. E. Projector Augmented-Wave Method. *Physical Review B* **1994**, *50*, 17953-17979.

(S3) Kresse, G.; Joubert, D. From Ultrasoft Pseudopotentials to the Projector Augmented-Wave Method. *Physical Review B* **1999**, *59*, 1758-1775.

(S4) Dunnington, B. D.; Schmidt, J. R. Generalization of Natural Bond Orbital Analysis to Periodic Systems: Applications to Solids and Surfaces Via Plane-Wave Density Functional Theory. *Journal of Chemical Theory and Computation* **2012**, *8*, 1902-1911.